

Comprehensive Comparison between the Experimental and Simulated Characteristics of the Mono-Crystalline Silicon Solar Cell Using SCAPS-1D



Salwa Nasser Ali^{1,□}, Mohamed Zahran^{1,2,3}, Ahmed A.Zaki Diab⁴

Abstract In this paper, a potassium hydroxide solution was used to etch the surface of the mono-crystalline silicon wafer, the sample was prepared at 0.33 Mol, solution temperature 82° C, 14 min etching time and by adding 1% of additive texturing material to KOH solution gives more homogeneity, the scanning electron microscope (SEM) indicated that. Moreover, a result using (scaps-1d) software has been presented to compare the experimental and simulated characteristics of the mono-crystalline silicon solar cell. Simulations were performed on silicon-based "p-n" solar cells. Moreover, a comparison between the simulated results and the experimental of the mono-crystalline silicon solar cell using scaps-1d has been presented. It can be concluded that the experimental and simulated values are in great agreement. The experimental results are $I_{sc} = 8.763A$, $V_{oc} = 0.629 V$, fill factor = 81.21%, and efficiency = 18.5%, while the simulation results are $I_{sc} = 8.729A$, $V_{oc} = 0.627 V$, fill factor = 83.16% and efficiency = 18.72%. When comparing the results obtained in the laboratory with the results extracted from the SCAPS-1D program, a great agreement has been found.

Keywords silicon solar cell, SCAPS-1D simulation, homogeneity, efficiency.

1 Introduction

In the current times, due to the increasing demand for energy and due to the tremendous development in the field of industry [1] the need has become necessary and urgent to search for new renewable and clean energy sources as an alternative to the use of fossil fuels [2] that are harmful to the environment, especially the ozone layer.

Renewable energy is obtained from natural sources that do not run out when used [3]. Examples of renewable energy are many and varied, including hydroelectric, wind, solar, etc. Solar energy is the third sustainable energy source used to generate energy after wind energy and hydroelectric energy [4] due to the ease of its immediate conversion into energy. Utilization has been expanding for renewable sources due to their abundance in nature, as they are environmentally friendly and non-polluting. It is expected that renewable energy will be used in a large and expanded manner, far exceeding the use of fossil fuels. Photovoltaic cells have an important role in the photovoltaic solar energy system. Solar cells produce electricity through the photoelectric effect, where sunlight generates electricity in certain materials by decomposing their external electrons. Mono-crystalline solar cells have played an effective and significant role in the technology of manufacturing silicon solar cells [5] due to their simplicity and advanced technology [6]. Many researchers in the field of manufacturing photovoltaic cells have conducted many researches and studies that improve the manufacturing process at a low cost, and higher efficiency [7-8]. In solar cells, silicon is the material that is utilized the most frequently. It is also abundantly found in nature as silicon dioxide in quartz and sand, where it is removed using carbon reduction. In actuality, silicon makes up roughly 26% of the earth's crust. Silicon optoelectronic devices are widely used in their manufacture [9]. It was found that one of the best proposed solutions to face the decrease in the traditional energy used is the use of sustainable renewable energy in electricity generation and industry [10], as well as to reduce human impact on the environment and increase energy independence [11-12]. Photovoltaic cells convert the enormous solar energy that it reaches the earth to benefit from electrical energy [13].

The efficiency of a solar cell depends on the absorption of photons and the electron-hole pairs produced in the space

Received: 14 February 2023/ Accepted: 29 March 2023
□Corresponding Author Name, Salwa Nasser Ali,
salwaaref2002@gmail.com

1. The joint National Egyptian-Chinese Renewable Energy Laboratory.
2. Ministry of Higher Education and Scientific Research.
3. National Authority for Remote Sensing and Space Sciences.
4. Electrical Engineering, Faculty of Engineering, Minia University.

charge region [14, 15].

The main objective of this study is to use scaps-1d to compare the experimental and simulated characteristics of mono-crystalline silicon solar cells. The verification of the simulation results through the experimental ones may assist authors in the future work for conducting other cases studied and providing new designs to improve the performance of solar cell. Both methods' I-V characteristics were compared with the points measured, and the results are indicated good agreement. Mono-crystalline silicon solar cell was used in the Egyptian-Chinese laboratory to conduct the experiment due to its advantages, which are:

- They perform better in low levels of sunlight, making them ideal for cloudy areas. They are perfect in low levels of sunlight because they work better in low light.
- They have the highest level of efficiency at 20-25% till now.
- They require less space compared to other types due to their high efficiency.
- According to the manufacturers, this type of solar cell has the longest lifespan, most of which have a 25-year warranty.

2 Structure of Solar Cell

Silicon solar cell is an electronic device that converts sunlight directly into electricity [16]. The mono-crystalline cell used in the experimental work consists of an absorber (P-layer) that is textured to form pyramids and a back surface field layer (P+) that is used to repel the minority carriers (electrons) in order to reduce the backside recombination of the absorber, a certain amount of aluminum diffuses into this region, forming a p+ region near the backside, that is, the aluminum backside field. This field pushes electrons from the back to the front, preventing the recombination of minority carriers on the back. [17], emitter (N-layer) that deposits to form the P-N junction, and an antireflection coating layer that is deposited on the front side to reduce the reflected light and front and back electrodes, as shown in Figure 1. Table 1. Simulated [p-n] junction parameters for silicon solar cells.

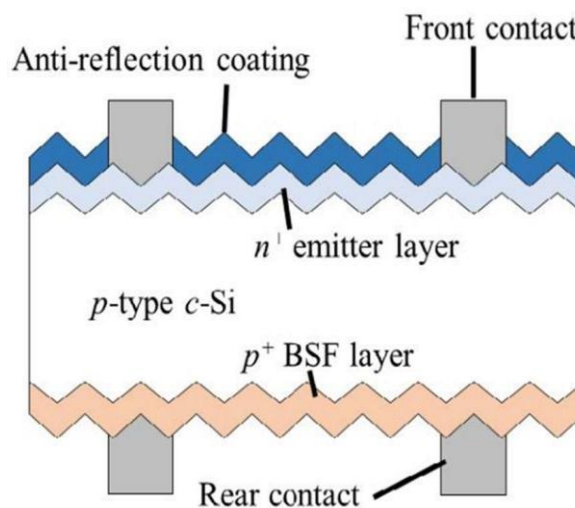


Fig1: Solar cell structure [16]

3 - Martial and Methods

The study focuses on a solar cell p-n structure based on silicon. Figure 2 shows the simulation process using the (SCAPS-1D) software. There are a lot of options in SCAPS-1D software, for example, the capability to work with amorphous cells (a-Si and micro-morphous Si) and crystalline solar cells (c-Si and GaAs, family) [18].

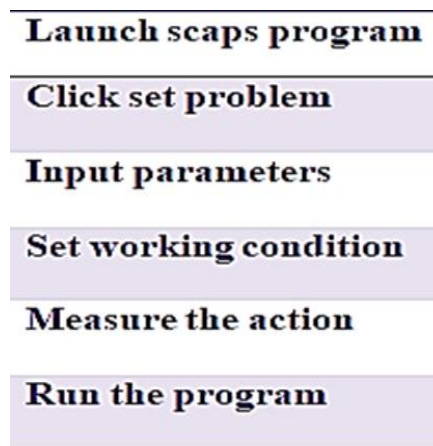
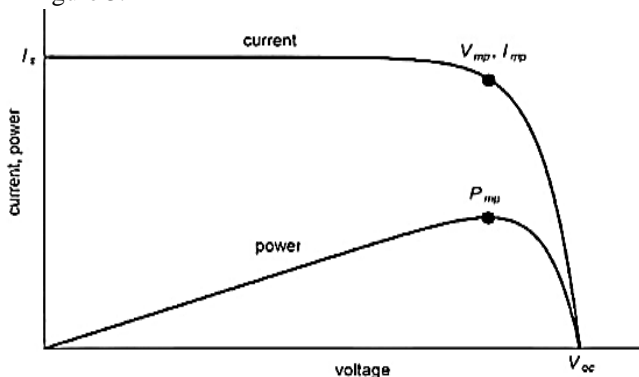


Fig 2: SCAPS working procedure

Table 1: Simulated [p-n] junction parameters for silicon solar cells.

Parameters	P+ BSF	p- bulk	p-si front	n-si
Thickness	5 μ m	170 μ m	5 μ m	0.5 μ m
Relative permittivity ϵ_r	11.68	11.68	11.68	11.68
Electron affinity χ_e (eV)	8	8	8	8
Band gap energy E_g (eV)	1.12	1.12	1.12	1.12
Electron mobility (cm ² .V ⁻¹ .s ⁻¹)	1400	1400	1400	1400
Hole mobility (cm ² .V ⁻¹ .s ⁻¹)	460	460	460	460
Effective conduction band Density N_C (cm ⁻³)	2.8 \times 10 ¹⁹	2.8 \times 10 ¹⁹	2.8 \times 10 ¹⁹	2.8 \times 10 ¹⁹
Effective valence band Density N_V (cm ⁻³)	1.04 \times 10 ¹⁹	1.04 \times 10 ¹⁹	1.04 \times 10 ¹⁹	1.04 \times 10 ¹⁹
Acceptor concentration N_A (cm ⁻³)	1016	1016	1016	0
Donor concentration N_D (cm ⁻³)	0	0	0	1016

The capacity of a photovoltaic cell to transfer the energy of photons that hit it is commonly referred to its conversion efficiency. Now, these measurements are uniform [19]. As a result, the makers test the solar cells at a constant temperature of 25°C under artificial light that simulates the solar spectrum AM1.5 (the total irradiance received on the Earth's surface at an altitude of 0° with an angle of 48°). At a constant temperature of 25 °C [20]. The PV module's cells got an average total power of 1000W/m² during testing [21]. Researchers are trying to boost the power density of solar cells [22]. The fill factor is a crucial quantity that is frequently used to certify the quality of a PV cell, a cell, or a PV generator from the current-voltage characteristic (FF). This coefficient shows the relationship between the highest powers a cell is capable of producing, P_{max} , and the power that the rectangle-shaped I-V curve can provide [23]. The peak power point of a solar cell can be used to describe it [24]. The largest rectangle gives the maximum power output of a cell, as shown in Figure 3.

**Fig. 3:** The fill factor.

Fill factor (FF) measures the junction quality [25], as shown in the following equation:

$$1-FF = (V_{mp} \times I_{mp}) / (V_{oc} \times I_{sc})$$

Fill factor is defined as the ratio of the maximum power (P_{max}) divided by the open circuit voltage (V_{oc}) multiplied by the short circuit current (I_{sc}).

$$2-P_{mp} = V_{oc} I_{sc} FF$$

Maximum power

It means the maximum power that can produce when working under standard test conditions, as the maximum power is the product of multiplying V_{mp} by I_{mp} .

Short circuit current (I_{sc}):

Is the maximum current that can generate in the case of zero or near zero resistance (under standard test conditions)

Open circuit voltage (V_{oc}):

It is the highest voltage at zero current. The value of Open circuit voltage increases with increased sunlight.

4. Experimental Work

Fabrication of mono-crystalline silicon solar cells deals with a set of chemical components and basic materials [26]. Figure 4 shows the different stages of manufacturing the mono-crystalline solar cell, which takes place in the Egyptian-Chinese factory for the manufacture of solar cells.

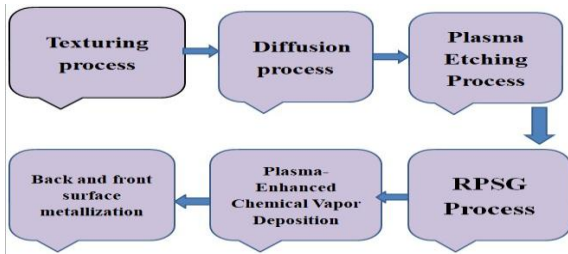


Fig. 4: Fabrication process of solar cell.

The coming wafers are P-type substrate doped boron. Wafers characteristics are shown in table 2.

Table 2: Wafer characterization.

Parameters	values
Area(mm ²)	156.75*156.75
Thickness(μm)	180+20/-10
Type&dope	P-Boron
Resistivity(Ω.cm)	0.5-1.5

4.1. Texturing process

The experiment was carried out at the Egyptian Chinese National Renewable Energy Laboratory. The apparatus used for texturing process is shown in figure 3, it consists of eight tanks (28 × 28) cm and a depth of (32) cm, were used as shown in the figure.



Fig. 5: Texturing machine.

After finishing the texturing process, the wafers should be dried using the dryer that is shown in figure 6. In the dryer machine, after a good rinsing of the wafers, the drying step will be done in the presence of nitrogen for five minutes at a temperature of 45°C.



Fig. 6: Dryer machine.

4.2. Diffusion process

To deposit the N-layer on the P-type substrate to form the P-N junction, the diffusion furnace is heated gradually (300, then 600, then the required diffusion temperature). After reaching the temperature, wait about 30 minutes for temperature stability shown in Figure 7.



Fig. 7: Boats on the paddle for loading inside the tube.

4.3. Plasma Etching Process

As the phosphorus-doped layer that is deposited during the diffusion process is formed at the edges of the silicon wafer so the cell is short-circuited so the edges must be removed during the plasma etching machine, as shown in Figure 8.



Fig. 8: Plasma etching machine.

4.4. RPSG Process

Removing phosphorus silica glass (RPSG), the wafers are placed in the first tank that contains deionized water and 3.1L of HF for 7 min at room temperature. Then wafers were placed serially in 3 tanks of deionized water at room temperature for 3min for cleaning.

4.5. Plasma-enhanced chemical vapor deposition (PECVD) furnace.

Deposition of the antireflection layer is carried out using silane (SiH_4) and ammonia (NH_3) and under a vacuum tube (low pressure) for 53 minutes and at the temperature of 380°C .

4.6. Back and front surface metallization (Screen Printing)

Print the impure silver (80% silver & 20% aluminum) on the back side of the cell to form bus bars that are used for welding the cells to each other to form the module. Then the cells are dried in the furnace at 150°C , and Aluminum paste is used in the backside of the cell. Then the cell is dried in the furnace at a temperature of 170°C ; after that in the third screen printer, the cells move on a conveyer belt, and the silver paste passes through a screen, as shown in Table 3.

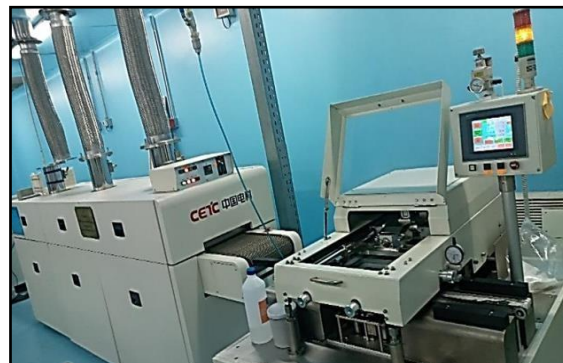


Fig. 9: Screen printer and its furnace.

4.7. The process of testing the solar cell efficiency

After finishing all fabrication steps, the cell should be tested to know its efficiency and electrical parameters to sort it for module soldering, minimize any possible mismatch losses in a module, and know the effects of the process parameters variation. I-V Cell Tester is shown in figure 10.

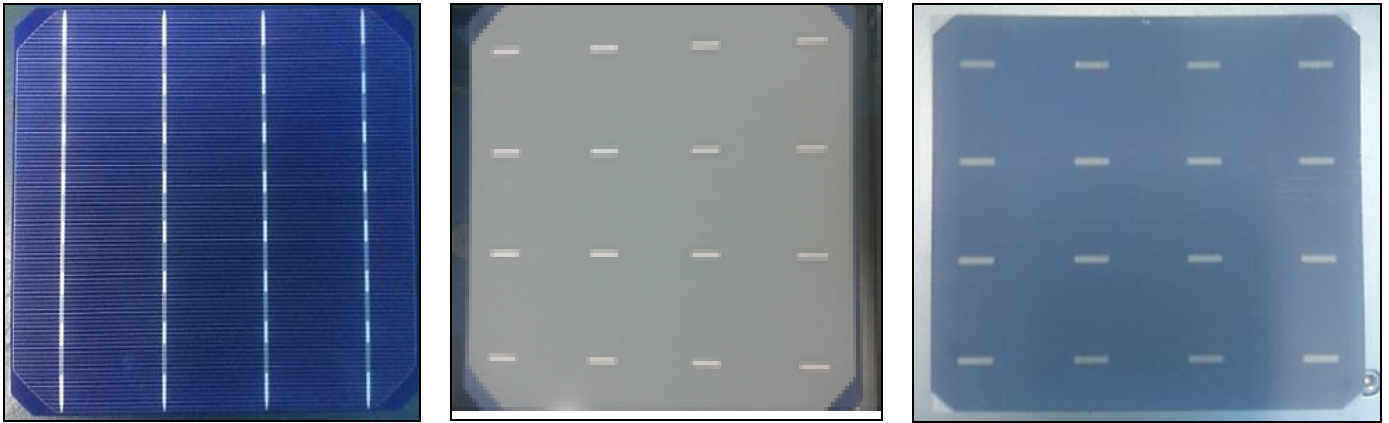
There are some conditions for testing, the testing temperature is 25°C , the air mass is 1.5, and the incident light power is 1000 W/m^2 .



Fig. 10: I-V Cell tester

Table 3: Wafer shapes after each printing stage.

A comparison of simulated and experimental silicon



Wafer shape after completing the third printing stage

Wafer shape after completing the second printing stage

Wafer shape after completing the first printing stage

solar references cells is shown in table 4; the experimental and simulated values are found to be reasonable

Table 4. Results from simulations and experiments.

Parameters	Experimental results	Simulation values
V_{oc} (V)	0.629	0.627
I_{sc} (A)	8.763	8.729
FF (%)	81.21	83.16
η (%)	18.59	18.72

The homogeneity of the silicon wafer samples is determined using a scanning electron microscope (SEM). The temperature used in the investigation at the Egyptian Chinese Laboratory for new and renewable energy is shown in Figure 11 at 82 degrees Celsius. One found that the pyramids consisted of large sizes with an average grain size (1.8μm). The pyramids were less reflective and more homogeneous at 82 degrees Celsius. It was found that the results obtained through the experiment are in great agreement with the results obtained by the researchers Ammar Mahmoud Al-Husseini et al. [27], and Wang et. al. [28].

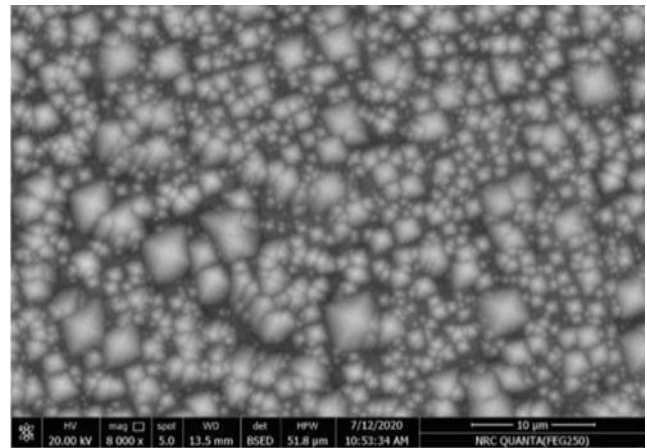


Fig. 11. SEM image of the silicon wafer surface after etching at 82° C

5- Results and Discussion

The experimental and simulated values are in decent agreement; it can be concluded that the experimental results are $I_{sc}=8.763$ A, $V_{oc}=0.629$ V, $FF=81.21\%$, and $\eta =18.5\%$. The Simulation results are $I_{sc}= (8.729)$ A, $V_{oc}=0.627$ V, $FF= 83.16\%$ and $\eta =18.72\%$. Figure 12. Show (I-V) curve, (P-V) curve of the experimental results of the mono-crystalline silicon solar cell, Figure 13 shows J-V characteristic of the silicon solar cell obtained from simulated results of the mono-crystalline silicon solar cell using mono-crystalline-1d.

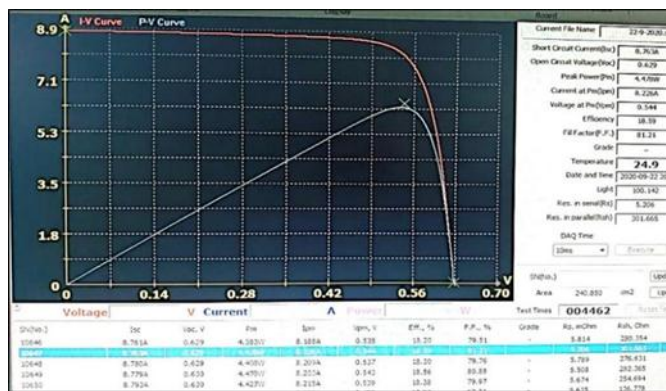
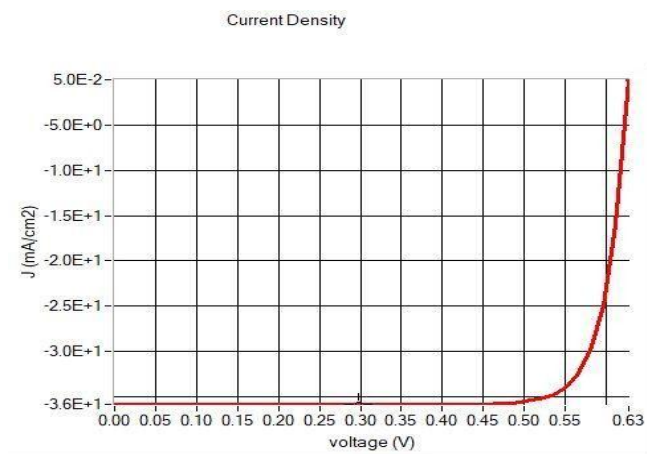


Figure 12. Silicon solar cell (I-V) and (P-V) curves.

Fig. 13. A silicon solar cell's J-V characteristic



5. CONCLUSION

In conclusion, silica solar cell optimization using numerical simulation using the SCAPS-1D program has been investigated. The study compared silicon solar cells that were simulated and those that were actually made. The installation process is carried out when the degree of a chemical reaction inside the basin is 82 ° C, as was discovered through the experiment to obtain homogeneous pyramids formed on the surface of the mono-crystalline solar cell, an appropriate amount of active substance is added, which is 230 ml. Additionally, a suitable quantity of (KOH) is added (0.3357 M0l), and the wafer is allowed to stay in the tank for 14 minutes. a comparison between the experimental and simulated results of the mono-crystalline silicon solar cell using scaps-1d.

References

- http://www.iea.org/publications/freepublications/publication/KeyWorld2014.pdf. (accessed July 2015).
- Edenhofer, O., Pichs-Madruga, R., Sokona, Y., Seyboth, K., Kadner, S., Zwickel, T., & Matschoss, P. (Eds.). (2011). Renewable energy sources and climate change mitigation: Special report of the intergovernmental panel on climate change. Cambridge University Press.
- Herzog, A. V., Lipman, T. E., Edwards, J. L., & Kammen, D. M. (2001). Renewable energy: a viable choice. Environment: Science and Policy for Sustainable Development, 43(10), 8-20.
- G. Masson, M. Latour, D. Biancardi, C. Winneker, Global Market Outlook for Photovoltaics until 2016, European Photovoltaic Industry Association, 2012.
- Han, K. M., Lee, H. D., Cho, J. S., Park, S. H., Yun, J. H., Yoon, K. H., & Yoo, J. S. (2012). Fabrication and characterization of monocrystalline-like silicon solar cells. Journal of the Korean Physical Society, 61(8), 1279-1282.
- Raval, M. C., Joshi, A. P., Saseendran, S. S., Suckow, S., Saravanan, S., Solanki, C. S., & Kottantharayil, A. (2015). Study of nickel silicide formation and associated fill-factor loss analysis for silicon solar cells with plated Ni-Cu based metallization. IEEE Journal of Photovoltaics, 5(6), 1554-1562.
- Murukesan, K., Kumbhar, S., Kapoor, A. K., Dhau, A., Saravanan, S., Pinto, R., & Arora, B. M. (2014, June). POCl 3 diffusion process optimization for the formation of emitters in the crystalline silicon solar cells. In 2014 IEEE 40th Photovoltaic Specialist Conference (PVSC) (pp. 3011-3013). IEEE.
- Schultz, O., Glunz, S. W., Riepe, S., & Willeke, G. P. (2006). High - efficiency solar cells on phosphorus gettered multicrystalline silicon substrates. Progress in Photovoltaics: Research and Applications, 14(8), 711-719.
- Koynov, S., Brandt, M. S., & Stutzmann, M. (2006). Black nonreflecting silicon surfaces for solar cells. Applied physics letters, 88(20), 203107.
- Malaoui, A.; Chahid, E. Accurate calculations of the Photovoltaic cells' intrinsic parameters: The physical and electrical properties of three generations of solar cells are investigated using developed methods. LAMBERT Academic Publishing 2022.
- Milojević, M., Nowodziński, P., Terzić, I., & Danshina, S. (2021). Households' Energy Autonomy: Risks or Benefits for a State?. Energies, 14(7), 2026.
- Chou, E., Southall, B. L., Robards, M., & Rosenbaum, H. C. (2021). International policy, recommendations, actions and mitigation efforts of anthropogenic underwater noise. Ocean & Coastal Management, 202, 105427.
- Xing, X., Sun, F., Qu, W., Xin, Y., & Hong, H. (2022). Numerical simulation and experimental study of a novel hybrid system coupling photovoltaic and solar fuel for electricity generation. Energy Conversion and Management, 255, 115316.
- Feng, D., Tervo, E. J., Vasileška, D., Yee, S. K., Rohatgi, A., & Zhang, Z. M. (2021). Spatial profiles of photon chemical potential in near-field thermophotovoltaic cells. Journal of Applied Physics, 129(21), 213101.
- Pandey, R., Madan, J., & Sharma, R. (2021). Enhanced charge extraction in metal-perovskite-metal back-contact solar cell structure through electrostatic doping: a numerical study. IEEE Transactions on Electron Devices, 68(4), 1757-1763.

- [16] Islam, R., & Abrar, M. M. (2020, October). Comparative Analysis of a Bifacial and a Polycrystalline Solar Cell Device Performances by Optimizing Effective Parameters Using PC1D. In 2020 International Conference on Smart Grid and Clean Energy Technologies (ICSGCE) (pp. 16-20). IEEE.
- [17] Chen, Y., Shen, H., & Altermatt, P. P. (2014). Analysis of recombination losses in screen-printed aluminum-alloyed back surface fields of silicon solar cells by numerical device simulation. *Solar energy materials and solar cells*, 120, 356-362.
- [18] A. Niemegeers, M. Burgelman, K. Decock, J. Verschraegen, Degraeve, SCAPS manual, May 2014.
- [19] Nozik, A. J. Quantum dot solar cells. *Physica E: Low-dimensional Systems and Nanostructures* 2002, 14, 115-120, [https://doi.org/10.1016/S1386-9477\(02\)00374-0](https://doi.org/10.1016/S1386-9477(02)00374-0).
- [20] Meng, Q., Wang, Y., & Zhang, L. (2011). Irradiance characteristics and optimization design of a large-scale solar simulator. *Solar Energy*, 85(9), 1758-1767.
- [21] Kadri, R., Andrei, H., Gaubert, J. P., Ivanovici, T., Champenois, G., & Andrei, P. (2012). Modeling of the photovoltaic cell circuit parameters for optimum connection model and real-time emulator with partial shadow conditions. *Energy*, 42(1), 57-67.
- [22] El Chaar, L., & El Zein, N. (2011). Review of photovoltaic technologies. *Renewable and sustainable energy reviews*, 15(5), 2165-2175.
- [23] Khelifaoui, N., Djafour, A., Ghenai, C., Laib, I., Danoune, M. B., & Gougui, A. (2021). Experimental investigation of solar hydrogen production PV/PEM electrolyser performance in the Algerian Sahara regions. *International Journal of Hydrogen Energy*, 46(59), 30524-30538.
- [24] Green, M. A. (1982). Accuracy of analytical expressions for solar cell fill factors. *Solar cells*, 7(3), 337-340.
- [25] López, C. S. P., & Frontini, F. (2014). Energy efficiency and renewable solar energy integration in heritage historic buildings. *Energy Procedia*, 48, 1493-1502.
- [26] Kempe, M. (2010). Evaluation of encapsulant materials for PV applications. *Photovoltaics International*, 9(NREL/JA-520-48926).
- [27] Al-Husseini, A. M., & Lahlouh, B. (2017). Research Article Silicon Pyramid Structure as a Reflectivity Reduction Mechanism.
- [28] Wang, Y., Luo, R., Ma, J., & Man, S. Q. (2015, August). Fabrication of the pyramidal microstructure on silicon substrate using KOH solution. In 2015 International Conference on Advanced Engineering Materials and Technology (pp. 302-307). Atlantis Press.